

0017-9310(94)00253-3

Heat and mass transfer of absorption process for the falling film flow inside a porous medium

RU YANG and DERMING JOU

Institute of Mechanical Engineering, National Sun Yat-Sen University, Kaohsiung, Taiwan, R.O.C.

(Received 25 April 1994)

Abstract—The heat and mass transfer for an absorption process taking place on a falling film flow in a porous medium is modeled by the Brinkman–Forchheimer extended Darcy equation and solved numerically. The solutions show that the transport rates are higher than that of a smooth film absorption process without a porous medium. The mass absorption rate increases with increasing solution flow rate, conductivity ratio and absorber pressure, and is optimum with porosity of 0.9 and conductivity ratio of 10. The correlations of dimensionless heat and mass transfer coefficients are given. These results will be valuable for the design of an absorption cooling system.

1. INTRODUCTION

The gas absorption process taking place on a falling liquid film has received much attention for its application in absorption heat pumps, chillers and air-conditioners. In these absorption machines, the refrigerant vapor from evaporator is absorbed by a falling film of an absorbent solution in an absorber, and then the absorbent solution is regenerated by releasing the refrigerant vapor in a regenerator (boiler). Since these absorption machines are driven mainly by low-grade energy, heat [1], rather than by high-grade energy, electricity, their application is especially interested in by areas where the electric power supply are limited. The performance of the absorption machine is controlled by the heat and mass transfer rates of the absorption process. Therefore, it is important to study the means of enhancing the heat and mass transfer rates of an absorption process.

Many studies had been addressed on a smooth film [2–4] or a wavy film [5, 6] absorption process. However, the wetting of a liquid on a smooth absorber-surface to form a film flow is difficult to maintain. A not well-wetted absorber-surface can drastically reduce the mass absorption rate due to the reduced effective heat and mass transfer area. In order to improve the wetting as well as to enhance the heat and mass transfer, some surface treatment is necessary. A possible means is to add a porous medium on the absorber-surface. In this study, the absorption process for an absorption process taking place on a falling film flow in a porous medium is considered. Since the study is motivated by the design requirement for an open-cycle absorption solar cooling system [7], aqueous lithium chloride solution and water are the absorbent and refrigerant, respectively.

2. ANALYSIS

A film of a liquid absorbent flowing down in a vertical porous thin film and absorbing the ambient gas (refrigerant vapor) is considered as the physical model. The problem can be formulated mathematically using the coordinate system defined in Fig. 1. The analysis is based on the following assumptions:

- (1) The liquid is filled (saturated) in the porous medium and the properties of the porous medium are assumed to be constant and homogeneous.
- (2) The liquid properties are assumed to be constant since the variations of temperature and concentration are presumed to be small.
- (3) The liquid film thickness is assumed constant since the rate of absorbed mass is much less than the mass rate of the main flow.
- (4) Equilibrium of the species exists at the liquid-vapor interface.
- (5) Diffusion is important only in the direction across the film since the Peclet number is practically large.
- (6) Diffusion-thermal effects are negligible [8].

The governing equation in accordance with these assumptions can be written as follows: the continuous equation is

$$\frac{\partial u}{\partial x} + \frac{\partial v}{\partial y} = 0. \quad (1)$$

The momentum equations can be modeled by the Brinkman–Forchheimer–extended Darcy equation since the Reynolds number of fluid flow in the porous medium is greater than 10 [9]. The equations can be written as

NOMENCLATURE

A	surface area
C	LiCl concentration [mass weight %]
C_1	Ergun constant
C_p	specific heat
D	mass diffusivity
Da	Darcy number, K/H^2
g	gravitational acceleration
h	heat transfer coefficient
H	film thickness
H_a	heat of absorption
h_m	mass transfer coefficient
k	conductivity
K	permeability
\dot{M}_{abs}	mass absorption rate per unit width
\dot{M}_s	liquid mass flow rate
Nu	Nusselt number, hH/k
Pr	Prandtl number, ν/α
P_v	absorber pressure
\bar{P}_v	normalized pressure, P_v/P_v^*
\dot{Q}	heat transfer rate
Re	Reynolds number, $4\Gamma_0/\nu$
Sh	Sherwood number, $h_m H/D$
T	temperature

u	x -direction velocity
v	y -direction velocity
x	coordinate parallel to the wall
y	coordinate normal to the wall.

Greek symbols

α_e	effective thermal diffusivity
Γ_0	mean volumetric flow rate per unit width of the absorber
ν	kinematic viscosity
ρ	liquid density
ϕ	porosity.

Subscripts

bulk	bulk mean values
eq	equilibrium condition
in	inlet quantities
out	outlet quantities
s	quantities associated with the solution
w	wall conditions.

Superscript

*	reference conditions.
---	-----------------------

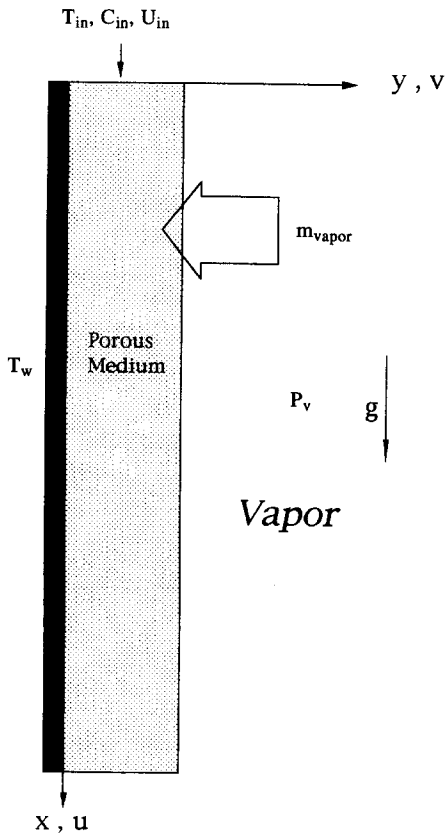


Fig. 1. The coordinate system.

$$u \frac{\partial u}{\partial x} + v \frac{\partial u}{\partial y} = -\frac{\phi^2}{\rho} \frac{\partial p}{\partial x} + \phi v \left(\frac{\partial^2 u}{\partial x^2} + \frac{\partial^2 u}{\partial y^2} \right) - \phi^2 \left(\frac{v}{K} + \frac{C_1}{\sqrt{K}} U \right) u + g\phi^2 \quad (2)$$

$$u \frac{\partial v}{\partial x} + v \frac{\partial v}{\partial y} = -\frac{\phi^2}{\rho} \frac{\partial p}{\partial y} + \phi v \left(\frac{\partial^2 v}{\partial x^2} + \frac{\partial^2 v}{\partial y^2} \right) - \phi^2 \left(\frac{v}{K} + \frac{C_1}{\sqrt{K}} U \right) v \quad (3)$$

where $U = \sqrt{u^2 + v^2}$ is the Darcian velocity, $C_1 = 1.75\phi^{-2/3}/\sqrt{150}$ is based on the Ergun model and $K = d^2\phi^3/150(1-\phi)^2$ is a Kozeny-Carman equation [10].

The heat and mass transfer equations are, respectively,

$$u \frac{\partial T}{\partial x} + v \frac{\partial T}{\partial y} = \alpha_e \frac{\partial^2 T}{\partial y^2} \quad (4)$$

$$\rho u \frac{\partial C}{\partial x} + \rho v \frac{\partial C}{\partial y} = \frac{\partial}{\partial y} \left(\rho D \frac{\partial C}{\partial y} \right) \quad (5)$$

where $\alpha_e = k/\rho_r c_{pf} = [\phi k_r + (1-\phi)k_p]/\rho_r c_{pf}$ is an effective thermal diffusivity for fluid-saturated porous medium [11]. The boundary conditions are

$$\begin{aligned} (1) \quad x = 0 \quad u &= u_{in} \\ &v = 0 \\ &T = T_{in} \\ &C = C_{in} \end{aligned} \quad (6)$$

$$(2) \quad y = 0 \quad u = 0$$

$$v = 0$$

$$T = T_w$$

$$\frac{\partial C}{\partial y} = 0 \quad (\text{non-permeable wall}) \quad (7)$$

$$(3) \quad y = H \quad \frac{\partial u}{\partial y} = 0$$

$$v = 0$$

$$-k \frac{\partial T}{\partial y} = \phi H_a \rho D \frac{\partial C}{\partial y}$$

$$C = C_{eq}(T, P_v). \quad (8)$$

The momentum equation is solved numerically by the SIMPLE algorithm [12]. Since the Peclet number is large in practical applications, the outflow boundary condition [12] is applied at the downstream boundary. The energy and concentration equations are solved by a finite difference method with a marching technique. Since variations of temperature and concentration are expected to be significant in the entrance region [4], the computational grid is chosen to be dense in that region. A total of 601 points in the x -direction and 51 points in the y -direction are found to be sufficient.

The major concern of the problem is the mass absorption rate that is evaluated by

$$\dot{M}_{abs} = \dot{M}_{s,out} - \dot{M}_{s,in}. \quad (9)$$

Since the salt is not volatile, its mass flow rate is constant, i.e.

$$\dot{M}_{s,in} C_{in} = \dot{M}_{s,out} C_{out} \quad \text{or} \quad \dot{M}_{s,out} = \dot{M}_{s,in} \frac{C_{in}}{C_{out}}. \quad (10)$$

Equations (9) and (10) are combined to obtain

$$\dot{M}_{abs} = \dot{M}_{s,in} \left[\frac{C_{in}}{C_{out}} - 1 \right]. \quad (11)$$

The mass transfer coefficient, h_m , is defined by

$$\dot{M}_{abs} = \rho h_m A [C_{in} - C_{eq}(T_w, P_v)] \quad (12)$$

where C_{eq} is the concentration when the liquid is in equilibrium with the wall temperature and the ambient vapor pressure. If the wall is sufficiently long, the liquid concentration will approach C_{eq} , which represents the lowest possible concentration of the absorption process.

The heat transfer rate is calculated by performing an energy balance over the entire control volume, which results in

$$\dot{Q} = \dot{M}_{s,in} h_{s,in} + \dot{M}_{abs} H_a - \dot{M}_{s,out} h_{s,out}. \quad (13)$$

The heat transfer coefficient, h , is defined by

$$\dot{Q} = hA [T_{eq}(C_{in}, P_v) - T_w] \quad (14)$$

where T_{eq} is the temperature when the liquid is in equilibrium with the inlet concentration and the ambi-

ent vapor pressure, i.e. T_{eq} represents the highest possible temperature of the absorption process.

3. RESULTS AND DISCUSSION

In this study, the base case conditions are chosen at: $C_{in}^* = 45\%$, $T_{in}^* = 35^\circ\text{C}$, $T_w^* = 30^\circ\text{C}$, $P_v^* = 8.5 \text{ mmHg}$, $Re^* = 58$, $k_p^* = 10$ and $\phi^* = 0.5$. One of the flow rate (i.e. Re), P_v , k_p or ϕ is varied at a time to study the individual effect of the parameter on the absorption rate. The bulk mean temperature and concentration of the solution film is defined, respectively, as

$$T_{bulk} = \frac{\int_0^H u T dy}{\int_0^H u dy} \quad (15)$$

$$C_{bulk} = \frac{\int_0^H u C dy}{\int_0^H u dy}. \quad (16)$$

Figure 2 illustrates the results for the interface and bulk mean temperatures of the liquid film along the absorber surface. The interface temperature is always higher than the bulk mean temperature owing to the heat of absorption released during the absorption process taking place on the interface. Both the interface and the bulk mean temperatures drop from the inlet temperature to a value close to the wall temperature due to the heat flux into the wall. A similar plot for the interface and the bulk mean concentrations is shown in Fig. 3. The interface concentration is much lower than the bulk mean concentration due to the absorption effect on the interface. In addition, the bulk mean concentration decreases slowly, which confirms that the mass absorption rate is much smaller than the flow rate of the main flow. Hence, assumption (3) can be justified.

Figure 4 illustrates the comparison of the present results for the standard case with previous results for smooth film absorption [2] and experimental data for wavy film absorption with 5% non-absorbables [13]. It can be seen that the absorption performance of the present case is better than that of the smooth film. Since the presence of the non-absorbables can degrade

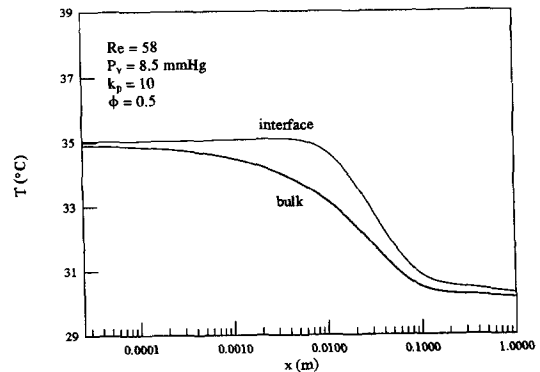


Fig. 2. The temperature of the interface and the bulk mean along the flow direction.

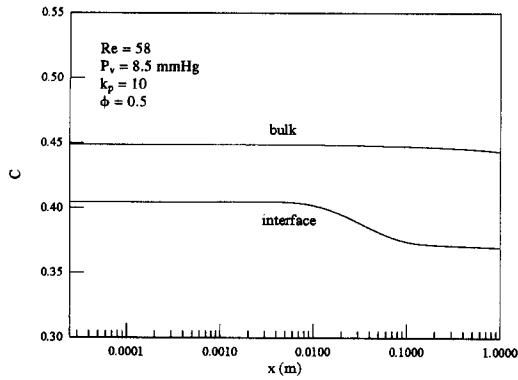


Fig. 3. The concentration of the interface and the bulk mean along the flow direction.

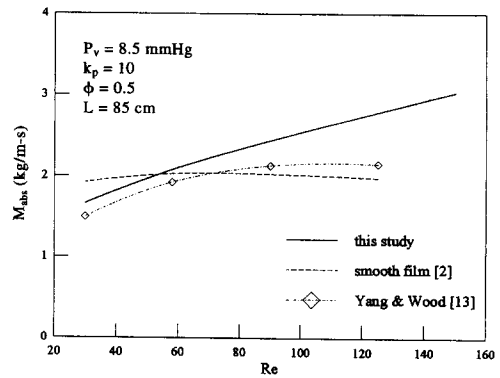


Fig. 6. The effect of Re on the mass absorption rate.

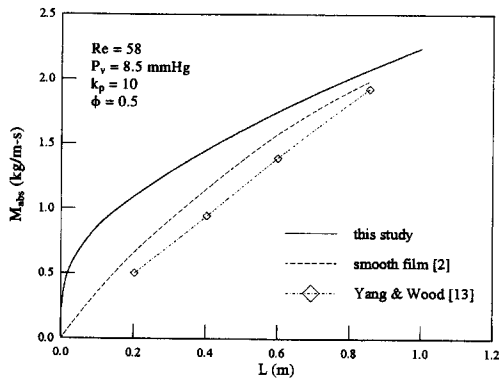


Fig. 4. The mass absorption rate varies with the absorber-length.

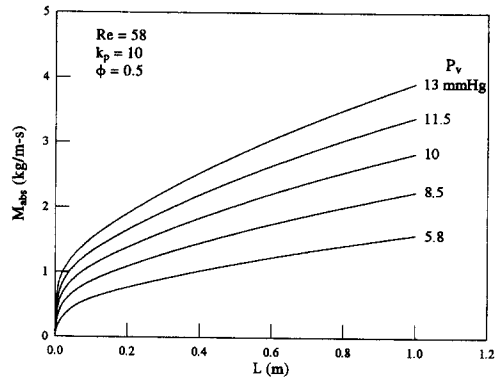


Fig. 7. The mass absorption rate varies with the absorber-length for various absorber pressures.

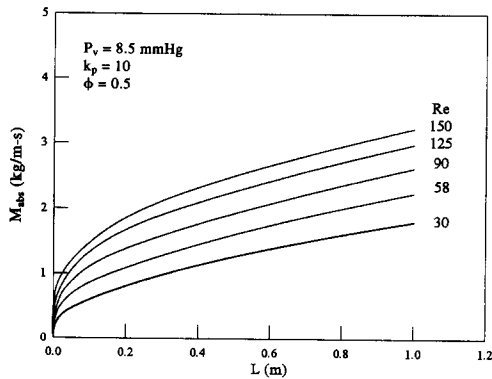


Fig. 5. The mass absorption rate varies with the absorber-length for various Re .

the absorption performance [3, 13], which is not considered in the present calculations, the experimental data shown in the figure are only for reference purpose.

The effect of the absorbent flow rate on the mass absorption rate for various lengths of absorber surface is shown in Fig. 5. Increase in the solution flow rate results in an increased absorption rate within the practical application range of Re from 30 to 150 for a fixed length of absorber-surface of 85 cm. The solution flow

rate effect on the absorption rate is shown in Fig. 6. The mass absorption flow rate increases almost linearly with increasing flow rate for the present study. In contrast, the previous smooth film solution shown in Fig. 6 indicates an optimum flow rate at $Re = 60$: then the mass absorption rate decreases with increasing flow rate. Therefore, the porous film absorption is preferred for the flow with $Re > 60$.

Figure 7 illustrates the effect of the absorber pressure on the absorption rate for various absorber-lengths. The absorber pressure corresponds to the saturation temperature of the evaporator, that is the temperature of the chilled water produced by the cooling system. The higher the evaporator temperature, the higher the absorption pressure. However, a low evaporator temperature is usually preferred in the design of a cooling system. The suitable design point for LiCl solution is 9°C which corresponds to an absorber pressure of 8.5 mmHg. As illustrated in Fig. 8, if the absorber is operated at an off-design point the absorption rate for the porous film absorption can be lower than that for a smooth film absorption.

The effect of conductivity ratio (k_p) on the absorption rate for various absorber-lengths is shown in Fig. 9. It can be seen that an increased conductivity ratio results in an increase in the absorption rate owing to the increased heat transfer rate into the wall. However,

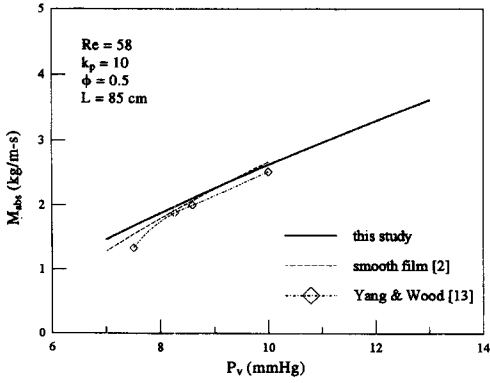


Fig. 8. The effect of P_v on the mass absorption rate.

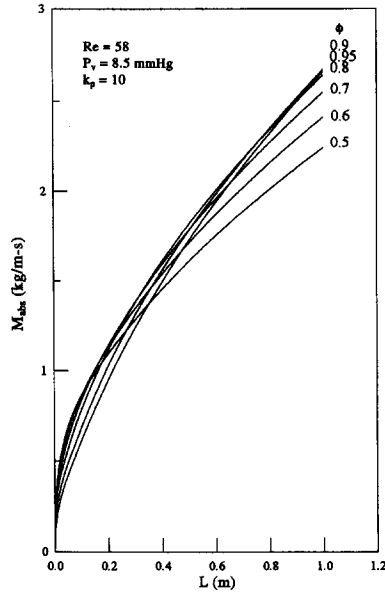


Fig. 11. The mass absorption rate varies with the absorber-length for various porosities.

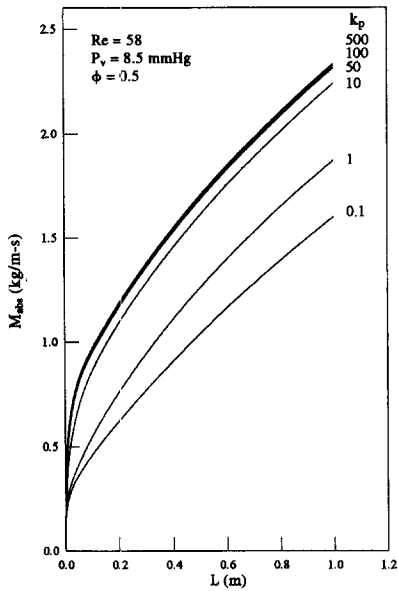


Fig. 9. The mass absorption rate varies with the absorber-length for various conductivity ratios.

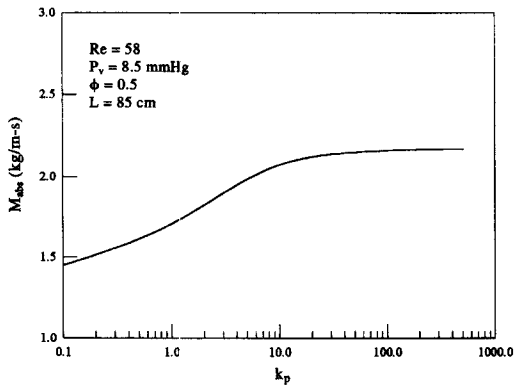


Fig. 10. The effect of k_p on the mass absorption rate.

when k_p greater than 10, the major transport resistance is due to that of the solution: a further increase in k_p has no effect on the absorption rate. This is clearly shown in Fig. 10.

Figures 11 and 12 show the effect of porosity on the absorption rate. It is seen in Fig. 12 that the absorption rate can be optimized with a porosity of about 0.9. Therefore, a practically reasonable porosity of 0.9 is a suitable choice for the porous film absorption applications.

In this study, the ranges of the parameters are the flow Reynolds number varying from 30 to 150, the absorber pressure varying from 7 to 13 mmHg, the conductivity ratio varying from 0.1 to 500, and the porosity varying from 0.5 to 0.95. The dimensionless heat and mass transfer coefficients can be defined, respectively, as

$$Nu = hH/k \tag{17}$$

$$Sh = h_m H/D. \tag{18}$$

The following correlations are obtained from the present study:

$$Nu = 0.0269 Re^{0.901} \overline{P_v}^{-0.0976} \phi^{0.0235} k_p^{0.0483} \tag{19}$$

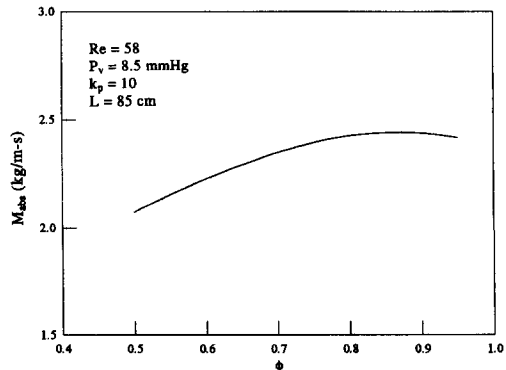


Fig. 12. The effect of ϕ on the mass absorption rate.

$$Sh = 1.175 Re^{0.756} \bar{P}_v^{0.069} \phi^{0.0371} k_p^{0.0492}. \quad (20)$$

4. CONCLUSIONS

This numerical study provides an absorber-design reference for the falling film absorption process in a porous medium. Although the application of porous media in a falling film absorption process is mainly to enhance the wetting conditions, the present study discovers that the absorption rate may also be enhanced by using porous media. The present results show that the mass absorption rate increases with increasing solution flow rate, conductivity ratio and absorber pressure, and is optimum with porosity of 0.9 and conductivity ratio of 10. The correlations of dimensionless heat and mass transfer coefficients are given. The present study, however, does not include the effect of non-absorbables. In practice, the presence of air residue acting as the non-absorbable gas in an absorber is unavoidable. Since air has a strong effect in depressing the absorption rate [3, 13], it is important to further study its effect on the falling film absorption process in a porous medium.

Acknowledgement—The authors gratefully acknowledge financial support from the National Science Council, Taiwan, in supporting this research under the contract NSC81-0401-E-110-541.

REFERENCES

1. J. B. Jones and G. A. Hawkins, *Engineering Thermodynamics*, p. 646. Wiley, New York (1986).
2. R. Yang and B. D. Wood, A numerical modeling of an absorption process on a liquid falling film, *Solar Energy* **48**(3), 195–198 (1992).
3. R. Yang and J. H. Chen, A numerical study of the non-absorbable effects on the falling liquid film absorption, *Wärme- und Stoffübertragung* **26**, 219–223 (1991).
4. G. Grossman, Simultaneous heat and mass transfer in film absorption under laminar flow, *Int. J. Heat Mass Transfer* **26**, 357–371 (1983).
5. R. Yang and D. M. Jou, Heat and mass transfer on the wavy film absorption process, *Can. J. Chem. Engng* **71**, 533–538 (1993).
6. K. Javdani, Mass transfer in wavy liquid films, *Chem. Engng Sci.* **29**, 61–69 (1974).
7. R. Yang and W. J. Yan, Simulation study for an open-cycle absorption solar cooling system operated in a humid area, *Energy* **17**(7), 649–655 (1992).
8. G. Grossman, Heat and mass transfer in film absorption, *Handbook of Heat and Mass Transfer*. Gulf Publishing, New York (1986).
9. K. Vafai and C. L. Tien, Boundary and inertia effects on convective heat transfer in porous media, *Int. J. Heat Mass Transfer* **34**, 195–203 (1981).
10. S. Ergun, Fluid flow through packed columns, *Chem. Engng Prog.* **48**, 89–94 (1952).
11. A. Bejan, *Convection Heat Transfer*, p. 353. Wiley, New York (1986).
12. S. V. Patankar, *Numerical Heat Transfer and Fluid Flow*. Hemisphere, New York (1980).
13. R. Yang and B. D. Wood, Experimental study of heat and mass transfer in laminar wavy film absorption with the presence of non-absorbable gases, *Chem. Engng Commun.* **125**, 77–90 (1993).